Development of Software-In-the-Loop Simulator and Hardware-In-the-Loop Simulator of AOCS Module for CubeSats

By Hirotaka SEKINE,[1)] Masahiro FUJIWARA,[1)] Satoshi IKARI,[1)] Takayuki HOSONUMA,[1)] Toshihiro SUZUKI,[1)] Riki NAKAMURA,[1)] Hajime ARAI,[2)] Yoshihisa SHIMADA,[2)] Tomofumi DOI,[2)] Hirokazu NAKAMURA,[2)] Shuhei MATSUSHITA,[1),3)] Akihiro ISHIKAWA,[1)] Ryu FUNASE,[1),4)] Shinichi NAKASUKA,[1)]

[1)] *Department of Aeronautics and Astronautics, The University of Tokyo, Tokyo, Japan*
[2)] *SEIREN Co., Ltd., Fukui, Japan*
[3)] *ArkEdge Space Inc., Tokyo, Japan*
[4)] *Institute of Space and Astronautical Science, JAXA, Sagamihara, Japan*

In recent years, more and more CubeSats have been launched, and higher attitude control accuracy has been achieved. However, CubeSat projects often face limited development time and human resources, leading to launches with insufficient reliable attitude determination and control algorithms. To enhance reliability in CubeSat development with limited resources, cost-effective, reusable Software-In-the-Loop Simulator (SILS) and Hardware-In-the-Loop Simulator (HILS) environments are necessary. Traditionally, ground testing environments have been mission-specific and difficult to reuse. We have developed open-source SILS and HILS environments to overcome this challenge. Using these reusable environments, we present simulation results for a 1U AOCS (Attitude and Orbit Control System) module developed by the University of Tokyo and Seiren, and JAXA. Furthermore, we discuss the attitude control results of the 6U satellite SPHERE-1 EYE, equipped with this module, confirming the successful performance of the algorithms during on-orbit operations. Our AOCS module is planned for integration into ONGLAISAT (ONboard Globe-Looking AI Satellite), scheduled for launch in 2024. We discuss potential developments in our ground testing environments concerning subsequent missions.

Key Words: CubeSats, Attitude Determination, Attitude Control, Software-In-the-Loop Simulator, Hardware-In-the-Loop Simulator

1. Introduction

In recent years, an increasing number of CubeSats have been launched, enabling the realization of various missions through these small satellites.[1)] Due to their smaller size compared to conventional large satellites, CubeSats can be developed more rapidly and cost-effectively, making them well-suited for the immediate demonstration of cutting-edge technologies on orbit and for tackling high-risk missions. Consequently, the missions carried out by CubeSats have become increasingly diverse, requiring more sophisticated attitude control in the CubeSat's AOCS (Attitude and Orbit Control System) to achieve the objectives of each mission.

Nevertheless, due to constrained development time, budget, and workforce, CubeSats are frequently launched with suboptimal reliability in attitude determination and control algorithms. Indeed, 29.6% of post-launch failures among 36 nano-satellites launched from Japanese universities and technical colleges are caused by AOCS-related issues, constituting the highest percentage among all subsystems.[2)] To effectively enhance reliability within restricted resources, a low-cost, user-friendly, and reusable testing environment is essential.

HILS (Hardware-in-the-Loop Simulator) and SILS (Software-in-the-Loop Simulator) are widely recognized as essential ground testing methodologies in satellite development. Numerous CubeSat missions have already implemented ground testing configurations for the verification of attitude control algorithms. In the case of MOVE-II (Munich Orbital Verification Experiment 2), which utilized a 1U CubeSat to test and verify the satellite bus, the construction of SILS and HILS environments enabled not only pre-launch testing but also facilitated ground testing prior to implementing on-orbit anomaly resolution after launch.[3)] For the KITSUNE (Kyutech standardized bus Imaging Technology System Utilizing Networking and Electron content measurements) mission, which employs a 6U CubeSat for the Earth observation with a 5-meter resolution, a SILS and HILS environment was established to verify the off-the-shelf MAI-400 product used in ADCS (Attitude Determination and Control System), successfully confirming the soundness of the algorithm prior to launch.[4)] However, many SILS and HILS environments developed thus far are mission-specific, making them difficult to reuse for subsequent projects. In particular, when development occurs within a closed environment, the cycle of modifications is limited, making it challenging to ensure reliability.

We developed highly reusable SILS and HILS testing environments to enhance satellite development. The SILS can simulate both the space environment and the communication between the Attitude On-Board Computer (AOBC) and components such as sensors and actuators. With its core features based on OSS (Open Source Software), the SILS can also be applied to other satellite development projects. Furthermore, we developed a HILS Interface (IF) Board to connect the AOBC and the simulator, enabling the verification of algorithms while accounting for communication time between the actual AOBC and simulated components. The input/output code, which em-

ploys the communication port of the PC, is integrated into the simulator, allowing for reuse in HILS tests of other AOCS modules.

This paper addresses the development of an efficient ground testing environment for the AOCS module collaboratively developed by the University of Tokyo and Seiren, and JAXA, and the validation of flight software through simulations. A 6U CubeSat SPHERE-1 EYE, which is equipped with the aforementioned AOCS module was launched in January 2023. The results of the on-orbit operation of the CubeSat are presented and compared with findings from ground testing. In Section 2, we provide an overview of the hardware and software of the AOCS module. Section 3 describes the satellite SPHERE-1 EYE, on which the AOCS module is actually installed. Section 4 introduces the details of SILS and HILS for the AOCS module. In Section 5, we will present the ground test results obtained using SILS and HILS, as well as the on-orbit performance of SPHERE-1 EYE. Finally, in Section 6, we provide a conclusion and future perspectives about our SILS and HILS.

2. Developed AOCS module for CubeSats

The AOCS module, which is the focus of tests in this paper, is shown in Fig 1. It has been developed by the University of Tokyo and Seiren, and JAXA. The target attitude control accuracy is 0.003 degrees (10 arcsec) at 1σ.[5)]

2.1. Hardware

The AOCS module weighs 1.2 kg and has 91 x 90 x 90 mm dimensions. The hardware configuration within the module is presented in Table 1. The sensors include rough gyro and magnetometers, fine magnetometers, sun sensors (SS), a fine gyro, a star tracker (STT), and a GPS receiver and antenna. The module is equipped with three magnetic torquer (MTQ) and three reaction wheels (RW) as actuators. Among these, the sun sensors, one of the two rough gyro and magnetometers, and one of the two fine magnetometers are mounted in separate locations of the satellite. The AOBC is adaptable to GPIO, UART, and I^2C interfaces.

Table 1. Component list.

Component	#	Interface	Voltage [V]
Rough gyro & magnetometers	2	I^2C	3.3
Fine Magnetometers	2	I^2C	3.3
Sun Sensors	4	I^2C	3.3
MTQ	3	GPIO	5.0
Fine Gyro	1	RS422	5.0
Star Tracker	1	RS485	5.0
Reaction Wheels	3	I^2C	7.5
GPS-R/A	1	LVTTL	3.3

2.2. Software

The software for the AOBC is Command Centric Architecture (C2A).[6)] C2A is a highly reconfigurable flight software for on-orbit operations, and its core functions are available as OSS.[7)]

The AOBC mode consists of seven distinct modes. The power states and attitude determination and control algorithms for each mode are shown in Figs. 2 and 3.

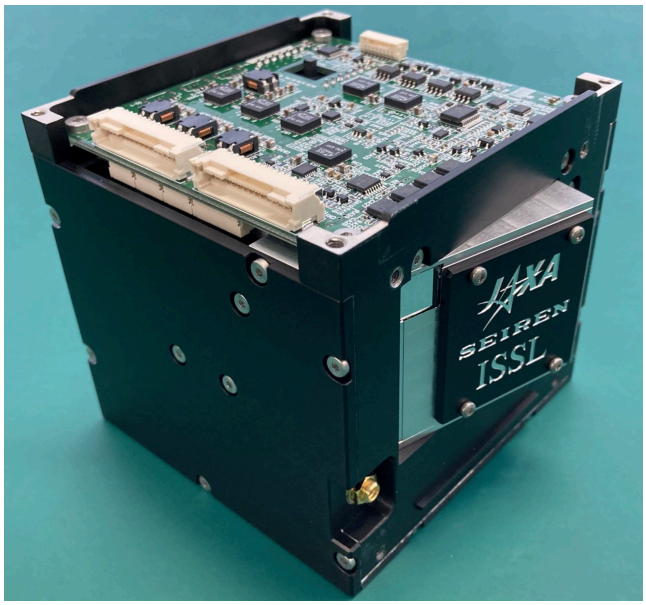

Fig. 1. AOCS module collaboratively developed by the University of Tokyo and Seiren, and JAXA.[5)]

C2A Mode	Power State (5V)						Power State (UNSTABLE)			
Name	Power Sensor	Rough GYRO	Rough MAG	Fine MAG	SS	MTQ	Fine GYRO	STT	RW	GPS
INITIAL	ON	ON/OFF	ON/OFF	ON/OFF	ON/OFF	ON/OFF	ON/OFF	ON/OFF	ON/OFF	ON/OFF
BDOT	ON	ON	ON	ON	OFF	ON	OFF	OFF	OFF	OFF
ROUGH_SUN_POINTING	ON	ON	ON	ON	ON	ON	OFF	OFF	OFF	OFF
ROUGH_THREE_AXIS	ON	ON	ON	ON	ON	ON	ON/OFF	OFF	OFF	ON/OFF
ROUGH_THREE_AXIS_RW	ON	ON	ON	ON	ON	ON	ON/OFF	OFF	ON	ON/OFF
FINE_THREE_AXIS	ON	ON	ON	ON	ON	ON	ON	ON	ON	ON

Fig. 2. The mode definition and switch status.[5)]

C2A Mode	Algorithm	
Name	Determination Algorithm	Control Algorithm
INITIAL	-	-
BDOT	Bdot damping	
ROUGH_SUN_POINTING	- Sun vector update/propagate - Angular velocity observation	- Sun vector and angular velocity FB with MTQ
ROUGH_THREE_AXIS	- TRIAD or QMethod with sun and mag sensor - Orbit and IGRF calculation	- Quaternion and angular velocity FB with MTQ
ROUGH_THREE_AXIS_RW	- TRIAD or QMethod with sun and mag sensor - Orbit and IGRF calculation	- Quaternion and angular velocity FB with RW - Unloading with MTQ
FINE_THREE_AXIS	- STT measurement - EKF attitude determination	- Quaternion and angular velocity FB with RW - Unloading with MTQ

Fig. 3. Attitude determination and control algorithms for each mode.[5)]

The initial mode is primarily used for ground testing. The Bdot mode and the Rough Sun Pointing mode are modes that can be used just after the satellite is released from the rocket without updating absolute time and orbit information from the ground. The Rough Three Axis mode and fine three-axis mode require updates of time and orbit information for attitude determination.

3. SPHERE-1 EYE

The AOCS module aforementioned was mounted onto a satellite called SPHERE-1 EYE and launched on January 3rd, 2023. The latest TLE (Two-Line Element) of the deployed orbit is presented in Table 2. SPHERE-1 EYE is a 6U CubeSat developed by the University of Tokyo, Sony Group Corporation, and JAXA, to capture images of the Earth and stars using a full-size camera. Overviews of the satellite are shown in Figs. 4 and 5.

Table 2. SPHERE-1 EYE's latest TLE published by NORAD on 20th April 2023.[8)]

SPHERE-1 EYE
1 55072U 23001BR 23110.78541380 .00016069 00000+0 83308-3 0 9994
2 55072 97.4880 171.3595 0014914 203.3426 293.8131 15.16151091 16371

Table 3. AOBC Fault Detection, Isolation and Recovery design.

Fault	Detection	Isolation	Recovery
Communication error	Component driver application	Turn off	Power reset
HW overcurrent	Current sensor	Latch	Latch release, power reset
SW overcurrent	Sensor monitor application	Turn off	Power reset
Outlier observed value	Filter application	Spike filter	-
Attitude control error	Mode manager application	Mode transition to Bdot	-
Calculation error	Each application	Assertion	-

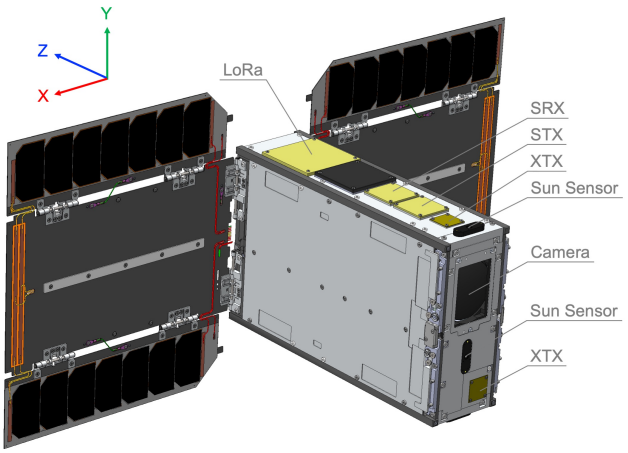

Fig. 4. The overview of SPHERE-1 EYE from +Y. ©Sony, UT

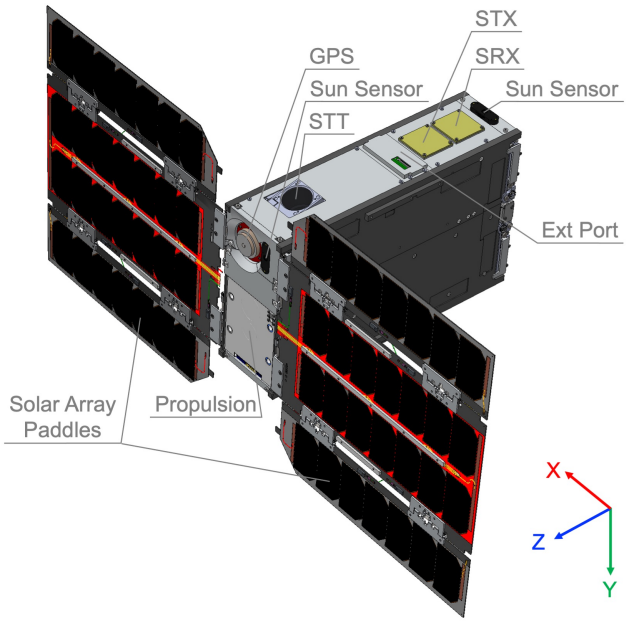

Fig. 5. The overview of SPHERE-1 EYE from -Y. ©Sony, UT

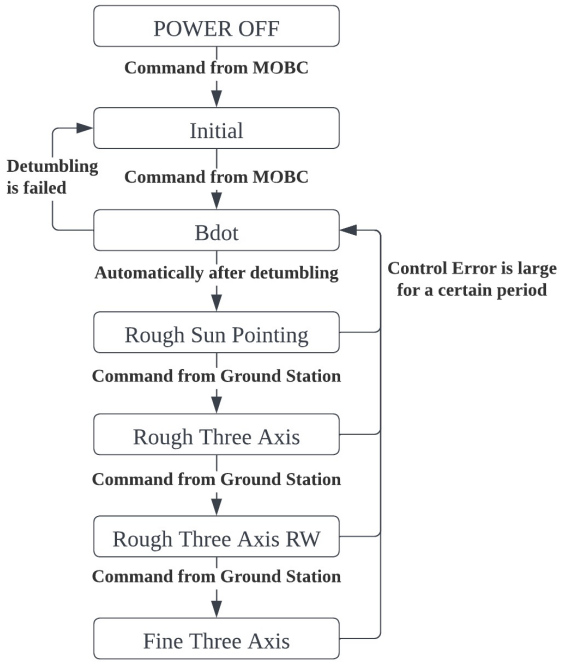

Fig. 6. AOBC mode transition diagram.

3.1. AOBC mode transition design

In this mission, a mode transition as shown in Fig 6 has been designed. When the AOBC is turned on, it immediately transitions from the START_UP mode to the Initial mode. Then it transitions from the Initial mode to Bdot mode by the command from the MOBC (Main On-Board Computer). The mode automatically transitions to the Rough Sun Pointing mode when the satellite's angular velocity remains below a certain value for a threshold duration. Subsequently, by sending commands from the ground, the satellite transitions through the Rough Three Axis control mode using MTQ, the Rough Three Axis control mode using RW, and finally, to the Fine Three Axis control mode. In Bdot mode, if the satellite's angular velocity continues to increase for a certain period, Bdot is interrupted, and the satellite automatically transitions to and stops in the Initial mode. On the other hand, if a large control error persists during the Rough Sun Pointing mode or any of the Three Axis control modes, the satellite automatically transitions to the Bdot mode.

3.2. FDIR desing

The FDIR (Fault Detection, Isolation, and Recovery) design of the AOBC is presented in Table 3. If a communication error between AOBC and a component is detected continuously for a certain period of time, the power to the component is reset. This communication error includes not only telemetry transmission and command reception but also CRC errors, checksum errors, and xxhash errors, depending on the component. In ad-

dition, overcurrents in sensors and actuators are protected by both hardware and software. As for hardware, the current sensor monitors the current flowing through each component and latches the circuit when the current exceeds a set threshold for a certain period of time on the order of sub-milliseconds, judging it as an overcurrent. Then, the power is turned off, and the latch of the current sensor is released. Finally, the power is turned on to attempt recovery. As for software, the current value measured by the current sensor is monitored, and if the current exceeds a set threshold for a certain period of time on the order of seconds, the power is turned off, judging it as an overcurrent. Then, recovery is attempted by turning the power back on. A filter application monitors telemetry from various sensors, and a spike filter detects and filters outlier values.

There are two FDIR algorithms related to attitude determination and control algorithms. The first is the mode manager application, which detects when the control error has been large for a long period of time and automatically transitions to a different mode. It transitions to the Bdot mode when the control error is large in either the Rough Sun Pointing mode or any of the Rough Three Axis modes. The second algorithm detects calculation errors. When a zero division or other errors occur in each application, it is detected, and an assertion is triggered.

Table 4. Overview of the ground test configuration.

	Flight SW	Components	Environment
Satellite	On AOBC	Real	Real
AOBC SILS	On S2E	S2E	S2E
AOBC HILS	On AOBC	S2E	S2E

Table 5. Recently updated features of S2E.[9)]

New Features	Details
Orbit calculation	- Kepler
	- Encke
Component emulation	- Antenna pattern
	- Structure change
Analysis tools	- Plot functions
	- Communication link budget calculation

4. Ground test simulator

In order to improve the reliability of the AOBC's attitude determination and control algorithms, we have developed SILS and HILS environments. The overall configurations of SILS and HILS are presented in Table 4.

4.1. Software-In-the-Loop Simulator

In our SILS, tests can be carried out within a computer using C2A on S2E (Space Environment Simulator). The core functions of S2E are available as OSS. Functional details are described in our previous paper,[5)] but subsequent updates are shown in Table 5. In addition to orbit propagation using the SGP4 algorithm, Kepler and Encke propagations have been added. Moreover, new features have been introduced for simulating satellite components, such as link budget calculations using antenna patterns and structural change calculations including mass, center of gravity, inertia tensor and residual magnetic moment (RMM). Furthermore, visualization tools have been developed to improve the efficiency of the analysis.

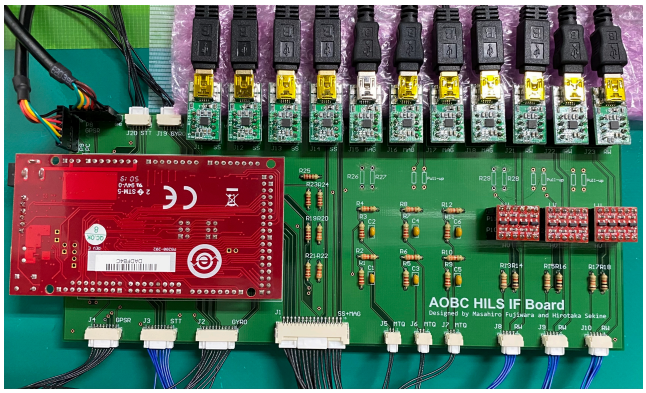

Fig. 7. HILS IF board.

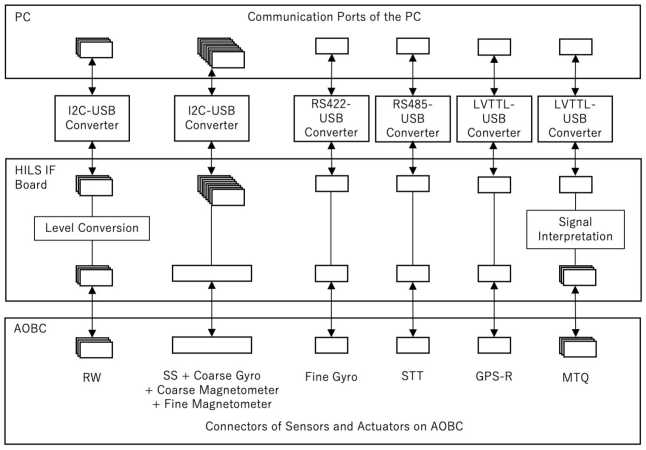

Fig. 8. The overview of HILS.

4.2. Hardware-In-the-Loop Simulator

HILS involves connecting the actual AOBC hardware with the S2E inside a computer. In HILS, realistic communication between the emulated components and the actual AOBC can be carried out, considering factors such as communication delays, and providing a more realistic simulation environment.

Our HILS focuses on verifying the AOBC's attitude determination and control algorithms, so the sensors are simulated within the S2E. The use of emulated sensors and actuators eliminates the need for expensive test facilities like a Helmholtz cage, solar simulator, star simulator, or air bearings, making testing more affordable and convenient. Additionally, functions for operating the computer ports necessary for telecommunication between emulated components on S2E and the AOBC have been developed within S2E and are publicly available as OSS.

We have also developed a HILS interface (IF) board to connect the PC ports and the AOBC. Images of the board is shown in Fig 7, and an overview of HILS is shown in Fig 8. This IF board allows for connector and voltage conversions. As shown in Table 1, the supply voltage for all I2C components except for RW is 3.3V. To standardize all USB-I2C converters connecting the PC port and the AOBC, the voltage of the RW line is converted from 7.5V to 3.3V. Furthermore, by reading the current output from the AOBC to the MTQ using a chipKIT Max32, it enables interpretation of the MTQ output on the PC side.

Table 6. The simulation condition for the ground test of mode transition from the Bdot mode to the Rough Sun Pointing mode.

Variable	Value
Start date	2022/10/01 00:13:00
Initial angular velocity [rad/s]	[0.01, 0.01, 0.01]
TLE	1 99999U 22999X 22274.00000000 .00000000 00000-0 00000-0 0 00005
	2 99999 097.5068 339.7118 0011775 245.9837 114.0163 15.15782335000010

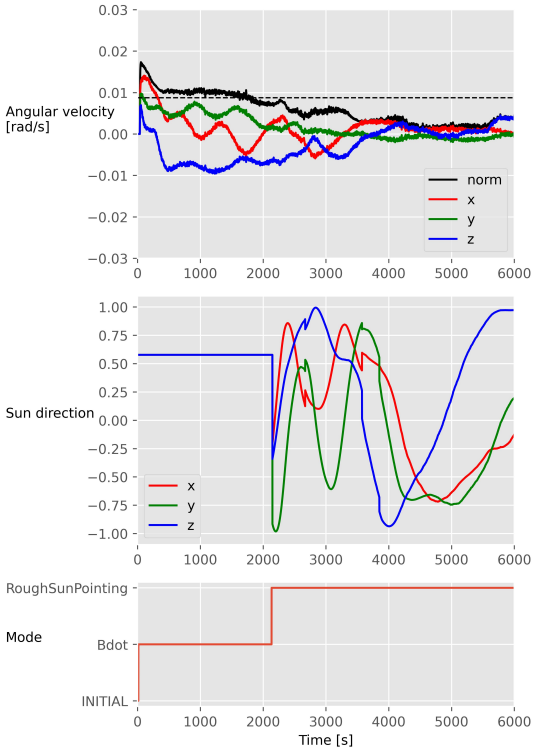

Fig. 9. Auto mode transition from the Bdot mode to the Rough Sun Pointing mode on SILS.

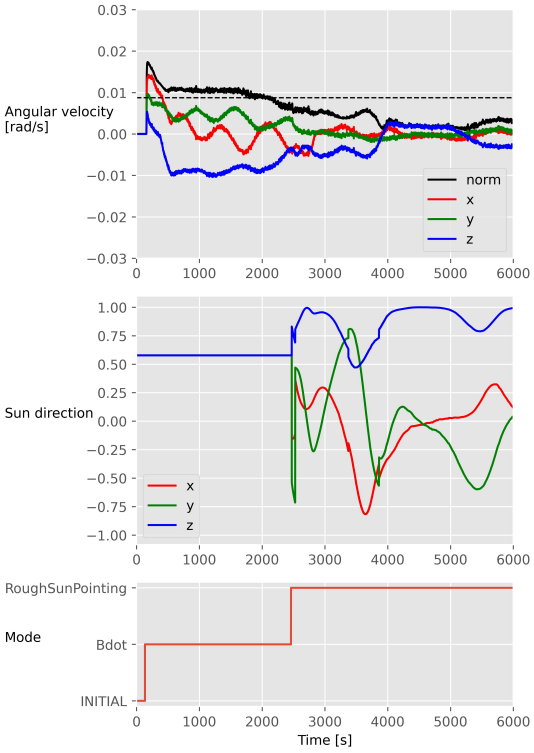

Fig. 10. Auto mode transition from the Bdot mode to the Rough Sun Pointing mode on HILS.

5. Ground Test Results and On-orbit Results

Before the satellite launch, SILS and HILS tests were conducted for each mode to verify the attitude determination and control algorithms. Additionally, by developing ground test facilities, the AOBC algorithm verification could be carried out even after the satellite was launched, allowing for thorough verification on the ground before implementing some operations on orbit.

5.1. Auto mode transition from the Bdot mode to the Rough Sun Pointing mode

5.1.1. Ground test results

We present automatic transitions from the Bdot mode to the Rough Sun Pointing mode, with the PZ (Positive Z-axis) of the satellite becoming sun-oriented. Common simulation conditions for SILS and HILS are shown in Table 6.

The results of the SILS tests are presented in Fig 9. The angular velocity drops below the threshold in about 1700 seconds from the start of the simulation, and the satellite transitions to the Rough Sun Pointing mode after the threshold duration. Sun orientation is achieved and stabilized after about 4000 seconds from the automatic mode transition.

The results of the HILS tests are shown in Fig 10. The angular velocity drops below the threshold in about 2000 seconds, and the satellite transitions to the Rough Sun Pointing mode after the threshold duration. Sun orientation is achieved and stabilized after about 1500 seconds from the automatic mode transition. Even considering the communication time between the components and the AOBC, it was confirmed that the satellite successfully completed the Bdot and the Rough Sun Pointing modes.

5.1.2. On-orbit results

Next, we present the results of the automatic mode transitions on orbit in Fig 11. While conducting the checkout, the automatic mode transition threshold was adjusted from the original 0.5 deg/s (0.009 rad/s) to 1.15 deg/s (0.02 rad/s). It was confirmed that the satellite's angular velocity norm is reduced by the Bdot mode on orbit, and the PZ sun orientation is achieved.

5.2. Mission attitude

Regarding the utilization of ground test facilities after the satellite launch, we present an example of attitude planning using SILS. As can be seen from the telemetry shown in Fig 12, it was confirmed that the attitude determination results on orbit closely follow the target attitude. Additionally, the absolute angular velocity for each axis was confirmed to be below 0.2 deg/s (0.003 rad/s), achieving safe attitude changes. The satellite successfully executed the planned attitude change, allowing for the capture of an image of eastern Japan, as depicted in Fig 13.

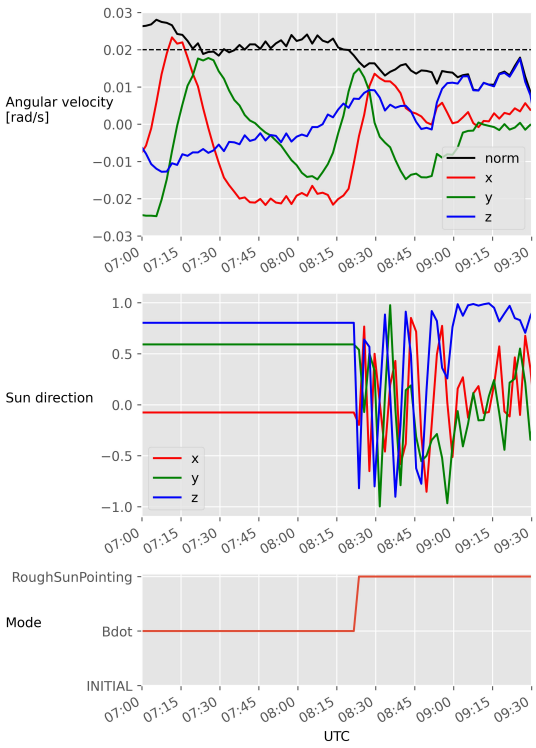

Fig. 11. Auto mode transition from the Bdot mode to Rough Sun Pointing mode on orbit on 22nd March 2023.

Fig. 12. Target attitude and estimated attitude during the mission operation.

5.3. FDIR

Several FDIR demonstrations have been confirmed on orbit. Additionally, as described in sections 5.3.1 to 5.3.3, it was discovered on orbit that there were some anomalies that the pre-launch implemented FDIR could not handle. Therefore, we addressed these anomalies utilizing the on-orbit reconfiguration feature of C2A to update the FDIR. We were able to conduct sufficient verification of new FDIR, using SILS on the ground. As a result, we greatly reduce the operational passes for implementing them on orbit.

5.3.1. SS telemetry error

When a telemetry error was detected in SSs, a power reset was performed as isolation and recovery. However, the telemetry error did not improve with the power reset alone, and abnormal values continued. As a result, another FDIR was triggered

Fig. 13. Eastern Japan captured by SPHERE-1 EYE.

that judged a control error if the sun was not detected for a certain period of time in the Rough Sun Pointing mode, and automatically transitioned to Bdot mode. This confirmed that the SS telemetry error and automatic mode transition FDIR were triggered as designed on the ground, but the telemetry error FDIR did not fully address the issue on orbit.

Subsequently, it was found that the SS telemetry error improved by resetting the buffer on the AOBC side. Therefore, by incorporating buffer reset into the FDIR recovery through C2A's orbit reconfigurable characteristic, automatic recovery could be achieved on orbit. As a result, the estimation of the sun's direction proceeded smoothly, and the three-axis attitude determination was also successfully accomplished.

This SS telemetry error was not confirmed in the AOCS module individual test on the ground. The SSs are attached to four sides: PZ/MZ/PY/MY. They are located away from the AOCS module, and there are some relay boards between AOBC and SSs. After the satellite assembly, it is possible that noise is more likely to occur on the SS communication line, including the possibility of noise affecting the telemetry error. We plan to investigate the cause and reflect it in the next satellite development.

5.3.2. AOBC hung up

After launch, the AOBC hung up about several times, and there was an issue where it did not send telemetry to MOBC despite current flowing. As shown in Fig. 14, all satellite positions were either in polar regions or within the South Atlantic Anomaly (SAA) regions. Furthermore, solar activity was intense in the early part of 2023, leading to a harsh radiation environment. Therefore, it is considered that the malfunction of the AOBC was due to radiation effects. After the AOBC hung up, we discovered that power resetting resolved the issue, allowing it to function normally. However, this reset process resulted in the loss of data written to the volatile memory. Therefore, we addressed this issue by registering the operational changes after launch as a command set in MOBC and setting up a system to automatically recover on orbit after a hang-up occurred.

5.3.3. RW anomaly

As shown in Fig 15, RWY's rotation telemetry sometimes froze, and the satellite began tumbling around the y-axis. The relationship between the satellite's angular velocity change and the rotation rate of RWY before it got stuck indicates that the rotation rate of RWY gradually came to a halt after the rota-

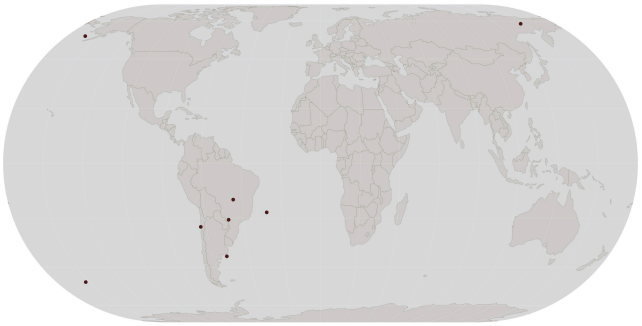

Fig. 14. AOBC hung up location.

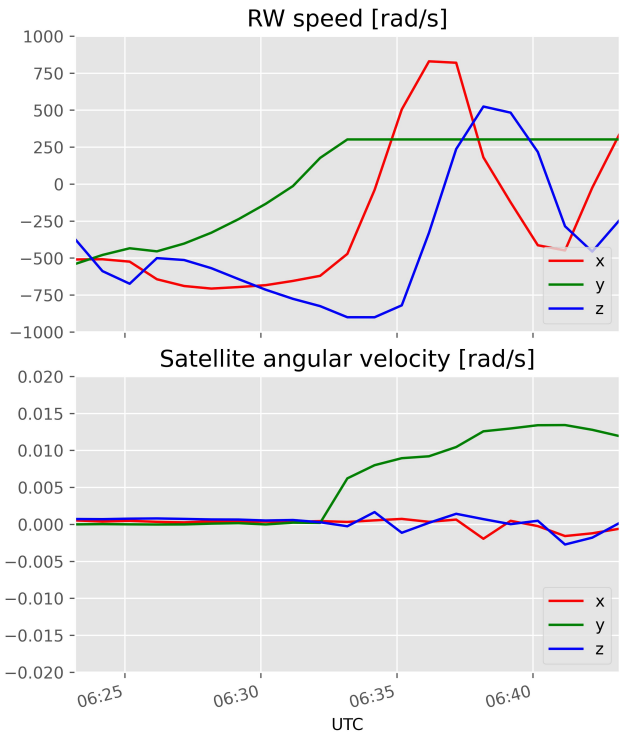

Fig. 15. RWY's rotation speed telemetry suddenly froze, and the satellite began tumbling around y-axis, on March 1st.

tion telemetry became fixed. In this case, the communication error of RWY was not detected. In addition, we did not have an FDIR to detect the sticking of the rotation rate of RWY, so initially, there was a long period of large control error when RWY's rotation stopped. There was no application to monitor RWY's rotation rate, and AOBC did not have the ability to add applications on orbit, so we addressed the issue as follows. We used an application to monitor the RWY's current value. When the time during which the current value is below a certain value continues for a certain amount of time on the order of minutes, the rotation of RWY is considered to be stopped. Then power reset is executed. With this new FDIR, the RWY began to move again within a few minutes after it stopped rotating. As shown in Fig. 16, we succeeded in shortening the period during which the control error became large due to the RWY malfunction. We found no anomalies in the AOBC circuit, and we suspect that the problem lies within the RW. Our assumption is that the cause of the anomaly is radiation.

The FDIR implemented on orbit this time to detect rotation stop from current values can accidentally activate during normal

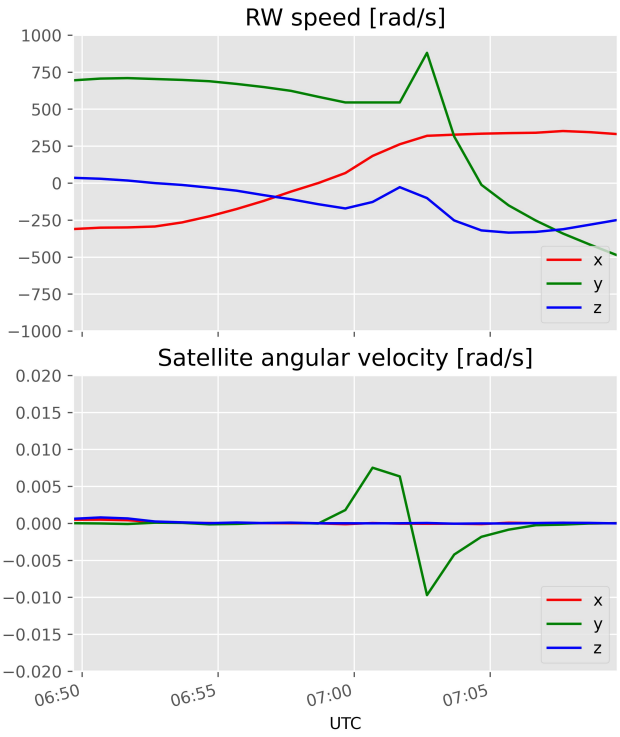

Fig. 16. RWY's rotation speed telemetry suddenly froze, and the satellite began tumbling around y-axis, on March 17th. Subsequently, the RWY power was reset by FDIR, and three-axis control was resumed.

times if the rotation rate happens to be small. Based on the results of this on-orbit demonstration, we would like to provide feedback on the FDIR design by incorporating a function to monitor value sticking.

5.4. Limitation of the ground test environment

We conducted numerous tests before launch using SILS and HILS, but there were two types of issues emerged on orbit that were not addressed before launch. The first type of issues were malfunctions that might be detected in the ground tests, for which an example is given in section 5.4.1. The second type of issues stemmed from component malfunctions. The issues outlined in sections 5.3.1 to 5.3.3 were all due to components, and were outside the scope of the SILS and HILS verification. Another example of this type of issue is given in section 5.4.2.

5.4.1. Abnormal torque command value

In the Rough Three-axis RW mode, there were often anomalies in the torque command values from AOBC to RW. The cause was the calculation of the target attitude. We were using a function where the satellite calculates its target attitude onboard, based on the propagated orbital information. There was a flaw in the assertion during this calculation process, causing the target attitude to become abnormal, which in turn resulted in incorrect command values for control. We addressed this issue by specifying the target attitude from the ground.

This issue was a calculation error that only occurred under specific orbital conditions, and it had not been detected during ground tests. However, the orbital conditions tested on the ground are limited. By updating to conduct SILS tests comprehensively and automatically, we would like to be able to confirm control under various orbital conditions in advance.

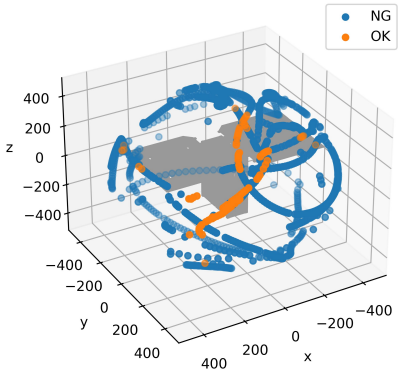

Fig. 17. Sun direction and STT attitude determination flag, under the condition that it is daytime and the STT exclusion angle is satisfied.

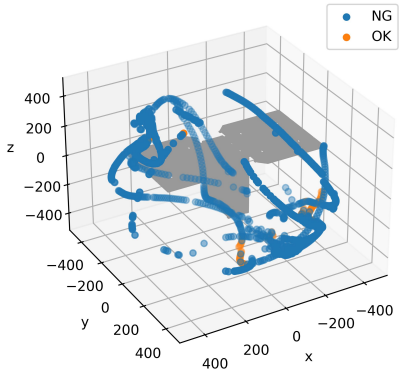

Fig. 18. The Earth direction and STT attitude determination flag, under the condition that it is daytime and the STT exclusion angle is satisfied.

5.4.2. Attitude determination of star tracker

In SILS and HILS, the solar and the Earth exclusion angles for STT and the angular velocity limit for attitude determination were simulated based on the specifications of the STT. However, after launch, the STT was unable to determine the attitude stably, despite meeting the exclusion angle and angular velocity conditions.

First, it became clear that during sunlight, there are directions in the body coordinate system where attitude determination is easier or more difficult depending on the direction of the sun and the earth. Figs. 17 and 18 depict the direction of the sun and the earth based on satellite's attitude determination using q-method. The period is limited to daylight, especially the sun is detected by any of the four sun sensors. The color shows that the STT was either able or unable to determine the attitude, respectively. As shown in Fig 5, the STT is installed on the MY side. It is clear that there are specific directions in the body coordinate system where attitude determination is easier or more difficult depending on the position of the sun and the earth. It should be noted that even in the PZ sun-pointing attitude where the sun hits the SAP vertically, the STT was unable to determine the attitude, possibly due to stray light. To address this issue, we plan to devise target attitudes during sunlight operation. We also plan to provide feedback on the system design rather than confining it to the AOCS module for the next satellite.

In the shadow, the period during which attitude determination can be performed is longer compared to those during sunlight, but it is not necessarily stable. It may be possible to improve this issue by adjusting the STT parameters.

6. Conclusion

We have developed reusable ground test environments, SILS and HILS. By using these to verify the attitude determination and control algorithms of the AOBC, we have successfully achieved the Bdot, the Rough Sun Pointing, and the Rough Three Axis attitude control in most time periods on orbit.

The construction of SILS and HILS has made it possible to easily verify algorithms even after the satellite has been launched. This allows us to confirm the validity of the target attitude and the integrity of the commands before sending them to the satellite on orbit, enabling more robust operations.

Based on the current operation, several new features have been identified that should be incorporated into the ground test system, including changes in power status and resulting changes in RMM. Additionally, the RW anomaly led to improvements in AOBC SW FDIR design and the STT anomaly prompted a review of the satellite system design. Additionally, the ONGLAISAT project, which aims to achieve a 2.8m ground resolution using TDI (Time-Delay Integration), is planned as the next mission.[10] We would like to apply the lessons learned from this mission to ONGLAISAT and future satellite missions.

Lastly, we are focusing on open-sourcing SILS and HILS. The core functions of c2a and s2e have already been published as OSS. We also plan to release the detailed parts, including attitude control algorithms and attitude simulation components, as OSS soon. We hope that the use of SILS and HILS in other projects will contribute to improved reliability of the ground test environment in the future.

Acknowledgments

The authors would like to thank all the project members for their contributions to the development of SPHERE-1 EYE.

References

1) Villela, T., Costa, C. A., Brandão, A. M., Bueno, F. T., and Leonardi, R.: Towards the thousandth CubeSat: A statistical overview, *International Journal of Aerospace Engineering*, (2019).
2) Tsuruda Y., Furumoto M., Miyata K., Cho M., Kuwahara T., Kitazawa Y.: Statistical Analysis of Lessons Learned from University Satellite Projects in Japan, 36th Annual Small Satellite Conference, Utah, U.S.A., SSC22-WKV-06, 2022.
3) Kiesbye, J., Messmann, D., Preisinger, M., Reina, G., Nagy, D., Schummer, F., et al.: Hardware-in-the-loop and software-in-the-loop testing of the move-ii cubesat, *Aerospace*, 6(12), 130, (2019).
4) Cordova-Alarcon, J. R., Jara-Cespedes, A. J., Withanage, D. C., Schulz, H., Orger, N. C., Kim, S., and Cho, M. Attitude Determination and Control System for the 6U CubeSat KITSUNE, 33rd International Symposium on Space Technology and Science, Oita, Japan, 2022-f-40, 2022.
5) Ikari, S., Hosonuma, T., Imamura, T., Suzuki, T., Fujiwara, M., Sekine, H., et al.: Development of Compact and Highly Capable Integrated AOCS Module for CubeSats, 33rd International Symposium

on Space Technology and Science, Oita, Japan, 2022-f-41, 2022.
6) Nakajima, S., Takisawa J., Ikari, S., Tomooka, M., Aoyanagi, Y., Funase, R., et al.: Command-centric architecture (C2A): Satellite software architecture with a flexible reconfiguration capability, textitActa Astronautica, 171, (2020), pp. 208–214.
7) GitHub, C2A core, https://github.com/ut-issl/c2a-core, (accessed April 23, 2023).
8) NORAD, celestrak, https://celestrak.org/NORAD/elements, (accessed April 23, 2023).
9) GitHub, S2E core, https://github.com/ut-issl/s2e-core, (accessed April 23, 2023).
10) Chen, Y., Huang, N., Shang, J., Lin, A., Lin, J., Ishikawa, A., et al.: Mission introduction of ONGLAISAT (ONboard Globe-Looking AI Satellite), 33rd International Symposium on Space Technology and Science, Oita, Japan, 2022-f-20, 2022.